*Proceedings of the 21st ICSMGE, Vienna, Austria, 14 – 19 June 2026. Pistrol, Adam & Schweiger (eds.)*
*Published by: ÖGG, Austrian Society for Geomechanics, Salzburg, Austria, ISBN 978-3-9503898-4-5*
*https://doi.org/10.53243/ICSMGE2026-2221*

# Thermal conductivity measurements for cable burial in the intertidal zone

**Bruno Stuyts,** Anis Kheffache
*UGent Geotechnical Institute, Ghent University, Belgium, bruno.stuyts@ugent.be*

Thijs Lanckriet
*Fluves NV, Ghent, Belgium*

Roel Vanthillo
*Marlinks NV, Ghent, Belgium*

ABSTRACT: Landfalls of offshore people cables are often planned in areas where sediment transport may influence the burial of the cable over time. The cable should retain sufficient cover throughout its operational lifetime to prevent it from becoming exposed. Measuring the depth of burial with conventional methods requires periodic surveys with amphibious survey vessels but changes in the sediment cover may be sudden due intense erosion (e.g. during storms). During the storms, the survey vessels cannot collect data in a safe manner. Measuring the temperature change of the optical fiber in the cable allows for the depth of burial of the cable to be derived using a 2D plane strain thermal model of the cable and the soil if the thermal conductivity of the soil is known. However, in the intertidal zone, seepage flows may occur between high and low tide which will lead to convective heat transport. This convective heat transport will lead to a more rapid lowering of the temperature of the cable. In this contribution, thermal laboratory measurements are reported which quantify the influence of seepage flow on the heat transport around a model cable. The measurements are used to determine an equivalent thermal conductivity for seepage flow conditions. Even though the heat transport will have a convective component, determining a representative equivalent thermal conductivity allows the 2D heat transport models to be used in the intertidal zone. Burial depths at the landfall locations can thus be determined, even during periods with adverse weather.

KEYWORDS: Paper template, instructions.

## 1 INTRODUCTION

Thermal geotechnical soil properties are fundamental to offshore power cable design as they directly control heat dissipation from the cable to the surrounding seabed environment. The thermal conductivity of marine sediments determines the maximum allowable current rating that can be safely transmitted through the cable without exceeding critical temperature limits (Carbon Trust, 2024).

Soil thermal conductivity variations significantly affect how much thermal insulation the backfill provides to a cable with a given burial depth, with deeper burial resulting in more heat generation in the cable. Understanding thermal properties enables engineers to predict cable operating temperatures under various loading conditions, ensuring compliance with international standards.

While the heat transfer is usually conductive for cables buried in deeper water depths. However, for cables buried in the intertidal zone, seepage flows may lead to convection and thus more efficient heat transfer.

Distributed Temperature Sensing (DTS) using optical fibers embedded in the cable has emerged as a alternative to periodic surveys for inferring cable burial depth (Ukil, Braendle and Krippner, 2011). When the thermal conductivity of the soil is known, the heat transfer equation can be inverted to obtain the burial depth which leads to a match with the measured temperature increase. When applying this technique to cables in the intertidal zone, any seepage flows will increase the heat dissipation from the cable into the surroundings.

This paper describes an experimental program which was set up to infer the influence of seepage flows on cable heating. First, the most common techniques for measuring thermal soil properties are described and their shortcomings for application in the intertidal zone are discussed. Next, the development of a bespoke testing bin based on the parallel hot wire method is presented. Finally, results from an experimental program on sandy soil from the North Sea subject to seepage flows of varying magnitude are presented and discussed.

## 2 THERMAL SOIL TESTING METHODS

### 2.1 *Empirical correlations*

In the absence of thermal soil testing, index test properties can be correlated with thermal conductivity. Farouki (1981) shows that moisture content has an important influence on the thermal conductivity of soils. It should be noted that this observation applied to partially saturated soils. For cohesionless offshore sediments, full saturation can be assumed and the in-situ moisture content may be difficult to establish.

The importance of mineralogy of the soil grains is also highlighted (Carbon Trust, 2024), with quartz having the highest thermal conductivity (7.7W/(m.K)) and clay minerals like kaolinite, montmorillonite and illite showing values between 1.4 and 2.8 W/(m.K).

### 2.2 *In-situ testing methods*

In-situ testing allows the thermal conductivity of the soil to be measured in-situ. The thermal CPT (T-CPT) is an add-on to the conventional CPT test which adds a temperature sensor on the cone (Vardon, Baltoukas and Peuchen, 2018). The technique is effective when the CPT rod generates sufficient friction to heat up the soil (at least 3°C temperature increase).

The advantage of in-situ testing is that the thermal properties are determined directly on the soil in its in-situ state. It should be noted however that backfill soils are affected by the trenching process and the thermal conductivity derived for undisturbed soil may not be representative for the soil on top of the cable.

### 2.3 *Laboratory testing methods*

The thermal needle probe (ASTM D5334-00, 2000) is one of the most common techniques for measuring soil thermal conductivity as it is a quick and inexpensive test. A heating element on the thermal needle leads to a temperature increase which is measured with a thermocouple. The thermal conductivity is derived from the quasi-linear proportion (in log-time space) of the temperature response of the soil. The downside of thermal conductivity measurements in cohesionless soil with the thermal needle probe is that undisturbed samples are hard to obtain. Any water draining from the sample during the sample retrieval will affect the results and full saturation is difficult to assure.

For the purpose of this study, thermal needle probe experiments were deemed insufficient, especially since full saturation and seepage flows needed to be achieved to simulate the conditions in the intertidal zone.

## 3 DEVELOPMENT OF A BESPOKE THERMAL TESTING BIN

### 3.1 *Measurement principle*

To simulate conditions in the intertidal zone, a bespoke thermal testing bin of 0.5m long x 0.4m wide x 0.5m high was developed. The large volume of soil ensures that there is significant offset between the heating wire and the edges of the bin. The solution of the temperature increase around a line source in homogeneous soil is given in Equation 1.

$$T = -\frac{q}{4\pi\lambda} E_i\left(\frac{-r^2}{4Dt}\right) \quad (1)$$

Where $T$ is the temperature increase due to the line source, $q$ is the thermal power of the source per unit length, $\lambda$ is the thermal conductivity of the soil, $D$ is the temperature distribution coefficient, $r$ is the offset between the line source and the temperature measurement location and $t$ is the time elapsed since the start of the heat-up. $E_i$ is the exponential integral which is given in Equation 2.

$$E_i(-x) = -\int_x^{\infty} \frac{e^{-u}}{u} du \quad (2)$$

The temperature distribution coefficient $D$ is related to the density $\rho$, the heat capacity $c_p$ and the thermal conductivity $\lambda$ of the soil as shown in Equation 3.

$$D = \frac{\lambda}{\rho \cdot c_p} \quad (3)$$

Figure 1 illustrates the theoretical solution of Equation 1 for six different sensor offsets and a thermal conductivity $\lambda$ of 1 W/(m.K) and a temperature distribution coefficient of 1e-7m$^2$/s. As the offset of the measurement point to the heating wire increases, the start of the temperature increase is delayed. Eventually, the measurements evolve to a line of constant slope in log-time space.

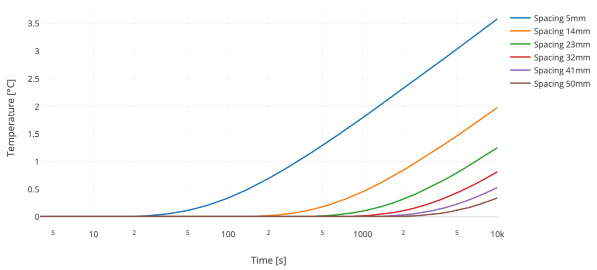


Figure 1. Theoretical solutions of temperature increase at different offsets from a heating wire.

When sensors are placed at a known offset from a heating wire, the theoretical solution from Equation 1 can be fitted to the measurement data. The thermal conductivity can be optimized to ensure a good fit. This is the theoretical basis for the parallel hot wire method according to NBN B62-202 (NBN, 1978).

### 3.2 *Bin dimensions and seepage flow generation*

The principle of generating seepage flows in the test bin is shown in Figure 2. A reservoir at a known height leads to a head difference between the water level in the bin and the piezometric height in the upper reservoir. A pump feeds to upper reservoir and there is an overflow from the test bin to a buffer tank. By varying the height of the upper reservoir, seepage flows of varying magnitude can be generated.

The head differences were selected to match typical flow velocities in the intertidal zone. Li, Boufadel and Weaver (2008) reported seepage flow velocities ranging between 1.1e-6m/s and 1.6e-5m/s for beach permeabilities from $10^{-4}$ m/s to $10^{-3}$ m/s, beach slopes from 3.16% to 31.6% and tidal amplitudes between 0.3m and 2m. It should be noted that the tidal amplitude in the Belgian North Sea can exceed 2m. Therefore, the maximum seepage flow velocity was increased to 1.5e-4m/s for the experiments.

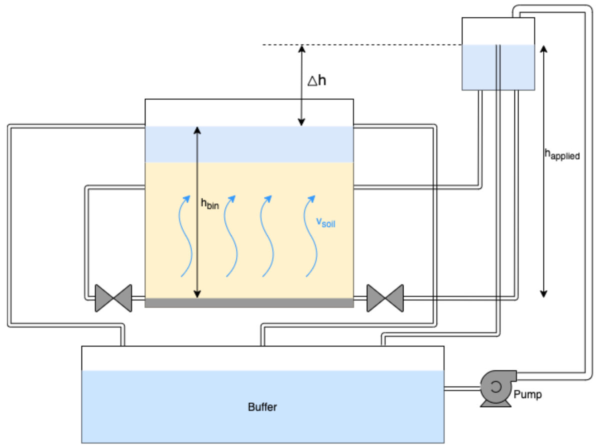


Figure 2. Schematic representation of the testing bin and the seepage flow generation.

The thermal testing bin is shown in Figure 3. Valves at the bottom allow the water to flow in and a gravel bed at the base of the bin, covered with a geotextile ensure even distribution of the flow across the whole cross-sectional area of the bin. The heating wire is positioned in the center of the bin, at 10cm from the bottom. Thermocouples are suspended on wires running parallel to the heating wire with offsets of 5, 10 and 20mm from the heating wire. For each offset, two different thermocouples were used to check consistency of the results.

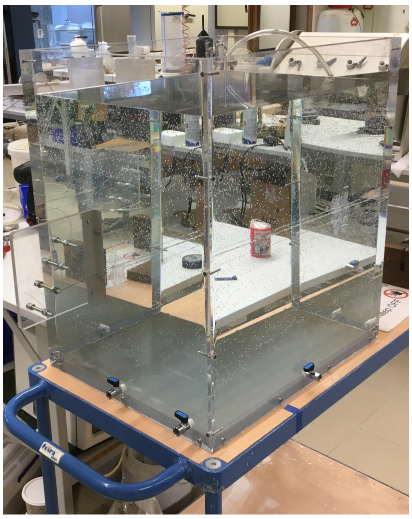

Figure 3. Picture of the thermal testing bin.

### 3.3 *Soil characterization*

The soil used for the testing was a fine to medium North Sea silica sand with limited fines content as shown in Figure 4. Index testing on the soil is described in Sun, Stuyts and Haegeman, (2024).

The permeability of the sand was tested with a constant head permeability test according to ASTM D2434-68 (2000) yielding values between 2.7e-4 and 3.2e-4m/s.

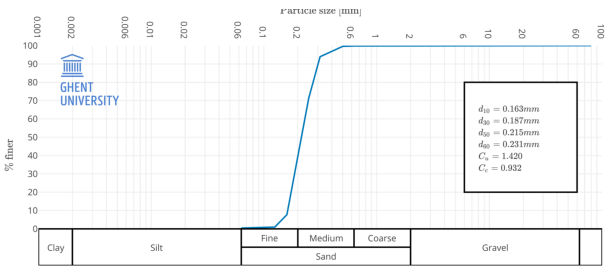


Figure 4. Grain size distribution of the sand.

### 3.4 *Test conditions*

The parallel hot wire test was performed for seepage flows between 0 and 1.5e-4m/s. The seepage flow was obtained by dividing the flow rate measured during the test by the horizontal cross-sectional area of the bin

The test was started by running a direct current through the heating wire. The heating power was derived from the applied voltage $V$ of 10.7V and the electrical resistance $R$ of the heating wire (0.3Ω) as shown in Equation 4. The heating power per unit length is derived by dividing the calculated power by the length of the heating wire in the bin (0.5m).

$$P = V^2/R \tag{4}$$

## 4 TEST RESULTS AND DISCUSSION

### 4.1 *Temperature build-up*

The temperature build-up for the heating wire and the thermocouples at three offsets is shown in Figure 5. As expected, the temperature increases start after a greater time when the offset of the thermocouple is increased. The results show relatively good consistency between the two thermocouples at the same offset. The theoretical model can be fitted to the sensors at the three offsets.

For a seepage flow of 2.1e-6m/s, this leads to an equivalent thermal conductivity of 20W/(m.K). Although this value leads to a good fit for the three sensor offsets, this value is much higher than the conventional range for thermal conductivity (1 to 4W/(m.K)). This shows that there is an important convective component of the heat transport.

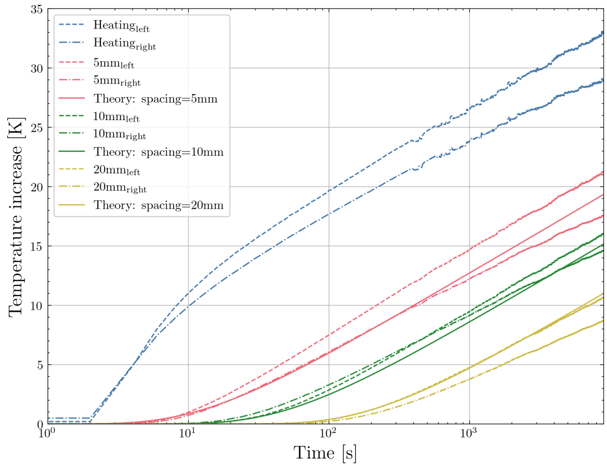


Figure 5. Fitting of an equivalent thermal conductivity to the temperature increase results for a seepage flow of 2.1e-6m/s.

### 4.2 *Effect of seepage flows*

Because the heat transport is not purely conductive, it was decided not to use the term thermal conductivity to present the test results. Instead, the temperature increase as a consequence of a given thermal power input was derived at a specific time.

Figure 5 shows that at 3600s, all thermocouples have reached a response which shows a linear increase in log-time space. The average temperature increase of each thermocouple pair was identified and the results are summarized as a function of the seepage flow in Figure 6.

As expected, an increasing seepage flow leads to a reduction of the temperature difference as the convective cooling effect starts to take over. This effect is more pronounced for the greater offsets, with the thermocouple at 20mm from the heating wire registering almost no temperature increase when the seepage flow becomes greater than 0.6e-4m/s.

Although some individual test results show slight anomalous behavior (e.g. the dip for the thermocouples at 5mm and 10mm offset for a seepage flow of 0.2e-4m/s), the overall picture reveals a consistent trend.

For low seepage flows (<0.1e-4m/s) the convective effective seems to be suppressed and a reduction of the temperature increase is only noticed for higher seepage flows.

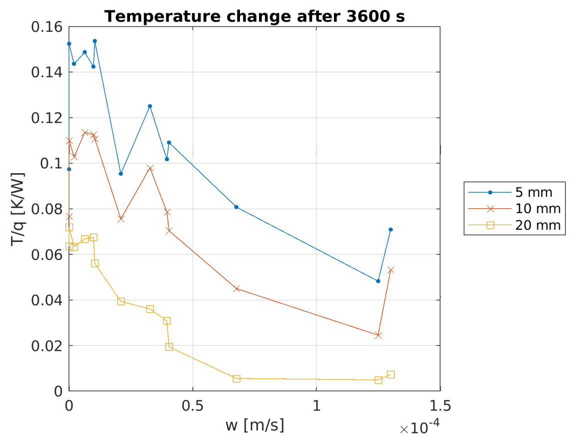


Figure 6. Reduction of temperature increase with increasing seepage flow

## 5 CONCLUSIONS

To measure the heat transfer around offshore power cables in the intertidal zone, where seepage flows can occur during tidal changes, a bespoke test setup was developed, based on the parallel hot wire method. By using a large volume of soil and several offsets between the thermocouple and the heating wire, consistent results were obtained which reveal the effect of seepage flows on the heat transfer around a long linear heat source.

The results show that when the seepage flow velocity passes a certain threshold, the convective component of the heat transfer manifests itself. When the seepage flow velocity becomes high enough, the convective component of the heat transfer dominated over the conductive component.

It should be noted that all results presented in this paper are for one type of sand with a relatively high permeability. In lower permeability soils, it is anticipated that the seepage flow velocities will be lower, and the convective component of the heat transfer will develop more slowly. Location specific testing is recommended in such cases.

When used in combination with a seepage flow analysis, the thermal properties derived from this study can inform the burial depth in the intertidal zone. Backfill of a given thickness in combination with a certain seepage flow velocity will lead to a temperature increase which can be measured with the optical fiber on the power cable (Distributed Temperature Sensing). This technique can be used to warn the cable operator when the cable becomes unburied.

## 6 ACKNOWLEDGEMENTS

The authors would like to thank the support of VLAIO De Blauwe Cluster through the DataBeach project.

The support of Filip Van Boxstael, Chief Technician of the Geotechnical Laboratory at UGent , in developing the experimental setup is gratefully acknowledged.

## 7 REFERENCES

ASTM D2434-68(2000), 2000. Standard Test Method for Permeability of Granular Soils (Constant Head) (Superseded with ASTM D2434-68(2006)). [online] Available at: <R:\Zotero\CA Standards\D2434.pdf>.

ASTM D5334-00, 2000. Standard Test Method for Determination of Thermal Conductivity of Soil and Soft Rock by Thermal Needle Probe Procedure (Superseded with ASTM D5334-08). [online] Available at: <R:\Zotero\CA Standards\D5334.pdf>.

Carbon Trust, 2024. Soil thermal properties for subsea cable design.

Farouki, O.T., 1981. Thermal properties of soils. [online] DTIC Document. Available at: <R:\Zotero\CA Technical references\1981 Farouki - Thermal properties of soils.pdf> [Accessed 6 June 2016].

Li, H., Boufadel, M.C. and Weaver, J.W., 2008. Tide-induced seawater–groundwater circulation in shallow beach aquifers. Journal of Hydrology, 352(1–2), pp.211–224. https://doi.org/10.1016/j.jhydrol.2008.01.013.

NBN, 1978. NBN B 62-202 Determination of the thermal conductance of building materials.

Sun, Y., Stuyts, B. and Haegeman, W., 2024. Statistical Uncertainty of Cyclic Resistance of Sand under Constant Volume Direct Simple Shear. In: 7th International Conference on Geotechnical and Geophysical Site Characterization. International Center for Numerical Methods in Engineering (CIMNE). pp.1779–1785. https://doi.org/10.23967/isc.2024.133.

Ukil, A., Braendle, H. and Krippner, P., 2011. Distributed temperature sensing: Review of technology and applications. IEEE Sensors Journal, 12(5), pp.885–892.

Vardon, P.J., Baltoukas, D. and Peuchen, J., 2018. Interpreting and validating the thermal cone penetration test (T-CPT). Géotechnique, pp.1–13.